Article:

Gao, J, Holden, J and Kirkby, M (2015) A distributed TOPMODEL for modelling impacts of land-cover change on river flow in upland peatland catchments. Hydrological Processes, 29 (13). pp. 2867-2879. ISSN 0885-6087

https://doi.org/10.1002/hyp.10408

A distributed TOPMODEL for modelling impacts of land-cover change on river flow in upland peatland catchments

Jihui Gao, Joseph Holden, Mike Kirkby
water@leeds, School of Geography, University of Leeds, Leeds, LS2 9JT, UK

Abstract

There is global concern about headwater management and associated impacts on river flow. In many wet temperate zones peatlands can be found covering headwater catchments. In the UK there is major concern about how environmental change, driven by human interventions, has altered the surface cover of headwater blanket peatlands. However, the impact of such land-cover changes on river flow is poorly understood. In particular, there is poor understanding of the impacts of different spatial configurations of bare peat or well-vegetated, restored peat on river flow peaks in upland catchments. In this paper, a physically-based, distributed and continuous catchment hydrological model was developed to explore such impacts. The original TOPMODEL, with its process representation being suitable for blanket peat catchments, was utilized as a prototype acting as the basis for the new model. The equations were downscaled from the catchment level to the cell level. The runoff produced by each cell is divided into subsurface flow and saturation-excess overland flow before an overland flow calculation takes place. A new overland flow module with a set of detailed stochastic algorithms representing overland flow routing and re-infiltration mechanisms was created to simulate saturation-excess overland flow movement. The new model was tested in the Trout Beck catchment of the North Pennines of England and found to work well in this catchment. The influence of land cover on surface roughness could be explicitly represented in the model and the model was found to be sensitive to land cover.

Keywords: blanket peat, flooding, peak flow, overland flow, vegetation cover

1 Introduction

Altering vegetation cover may affect river regimes due to changes in the overall water balance (inputs versus outputs) and also because of changes to flowpaths for water to the river channel. Understanding the impact of vegetation cover and management on the shape of storm hydrographs and the magnitude of flow peaks is vital to support land management decisions (Wheater and Evans, 2009).

Peatland landscapes are particularly sensitive to slight shifts in local hydrology or chemistry in which can alter species composition and hence surface cover (Bragg and Tallis, 2001). Peatlands cover around 3% of the Earth's land surface (Immirzi *et al.*, 1992) and as peatlands are more likely to form in regions with high precipitation excess, they often form in upland areas of the temperate and boreal zones (Gallego-Sala and Prentice, 2013). Large areas of the UK uplands are covered by blanket peat. Blanket peatlands typically have shallow water tables (Price, 1992; Evans *et al.*, 1999), and hence the potential for peat to store additional fresh water and act as a buffer to flooding may be very limited (Holden and Burt, 2003; Holden, 2005). Thus a little rainfall can cause rapid saturation of the peat and lead to the generation of saturation-excess overland flow or rapidly-flowing near-surface throughflow and these flows may dominate the river hydrograph during storm events (Holden and Burt, 2002). The river regime of blanket peatlands tends to be very flashy with rapidly rising hydrographs, high flow peaks and very little baseflow (Price, 1992; Evans *et al.*, 1999). There are concerns that land management interventions in upland peatlands in the UK may increase flood peaks (e.g. Parrott *et al.*, 2009; Wheater and Evans, 2009; Hess *et al.*, 2010). However, given that these systems are already very flashy in nature it is not clear what impacts such interventions might have. There is also the related problem of the spatial distribution of management interventions. As noted by Holden (2005), the same intervention may both theoretically increase and decrease the flood peak in the main river channel depending on how the intervention affects the timing of water delivery and its synchronicity from different parts of the catchment. There is therefore a need to understand such issues and assess them to support environmental decision making.

In many areas of the UK uplands there has been a history, over at least the last 60 years, of vegetation loss attributed to vegetation burning, overgrazing, atmospheric pollution and other interventions (Bower, 1962; Evans, 2005; Holden *et al.*, 2007b). A loss of a dense understory of

Sphagnum or the complete loss of surface vegetation altogether may lead to changes in water movement over peatland surfaces. It is thought that downstream discharge from peatlands might be sensitive to surface vegetation cover change (Holden *et al.*, 2008; Grayson *et al.*, 2010; Ballard *et al.*, 2011; Lane and Milledge, 2013). Vegetation cover and associated surface roughness could be more important to flow peaks in many headwater peatlands than change brought about by other management interventions such as drainage for which studies have often resulted in equivocal conclusions (Holden *et al.*, 2004). *Sphagnum* is associated with a much greater surface roughness than bare peat and it therefore has an ability to significantly slow down the velocity of water movement (Holden *et al.*, 2008). Peatland restoration efforts are underway across many degraded upland landscapes and these often seek to revegetate bare peat (Parry *et al.*, 2014). Practitioners are very keen to understand whether such revegetation has an impact on river flows (e.g. IUCN, 2011). Thus, we need a tool to evaluate the impact on river flow peaks of changes to, and the spatial distribution of, land cover types in headwater peatlands.

TOPMODEL was originally developed by Beven and Kirkby (1979), and initially employed in UK small catchments (Beven *et al.*, 1984). The model is considered as a set of conceptual tools which can be utilised to model the hydrological processes (especially the dynamics of surface and subsurface contributing areas) in a relatively simply way (Beven, 1997). TOPMODEL has been treated as a standard model for hydrological analysis in many parts of the world (e.g. Franks *et al.*, 1998; Lamb *et al.*, 1998; Güntner *et al.*, 1999; Peters *et al.*, 2003).

The assumptions of TOPMODEL (Beven and Kirkby, 1979) fit the case of blanket peat catchments well, in which river flow is dominated by surface or near-surface flow and there is a rapidly declining rate of flow in the top few centimetres of the soil profile (Holden and Burt, 2002). Although there is flow at depth in blanket peat, it makes negligible contribution during streamflow peaks (Evans *et al.*, 1999; Holden and Burt, 2003). The model is felt to be widely applicable in catchments dominated by shallow subsurface flow and overland flow, and the limited number of parameters is another advantage of TOPMODEL. However, the model is not spatially distributed and has only a very simplified component to represent overland flow movement, so the model cannot describe the impacts of different distributions of vegetation cover change and their impacts on surface flow and downstream river flow. Thus, while TOPMODEL is suitable for peatlands, it needs to be modified into a distributed model in order to be able to simulate and test different spatial configurations of land-cover change impacts on river flow.

The main purpose of this paper is to develop a model, based on the original TOPMODEL, which can simulate the impact of land-cover change in upland peat catchments on downstream hydrographs. To achieve this aim, there are two major tasks for model development. First, a spatially-distributed model structure is needed to identify and handle the variety of spatial patterns of land cover in peatland catchments. The other prime assignment is to establish an overland flow movement module which can distinguish between the various influences of land cover on surface water delivery on hillslopes because the majority of stream discharge during high flow events in blanket peatlands is derived from surface flow (Holden and Burt, 2003). We test the new distributed model with real storm events in the Trout Beck catchment of the North Pennines in UK and also compare model results to those from the original TOPMODEL.

2 Development of a distributed TOPMODEL

TOPMODEL was a continuous lumped or semi-distributed deterministic hydrological model when developed by Beven and Kirkby (1979). It is based on a simple theory of hydrological similarity of points in a catchment, by which the index of hydrological similarity is determined from the topographic index of Kirkby (1976) and provides good computational efficiency. The movement of subsurface flow was calculated together with overland flow in the original version of the model due to its lumped structure. Overland flow was generated for each value of the topographic index, and combined using a constant overland flow velocity. Here we develop an approach for distributing the model, calculating hydrological behaviour individually in every cell from Digital Elevation Model (DEM) data. The TOPMODEL rationale can be applied and hydrological equations downscaled from catchment scale to cell scale (probably 10-1000 m^2). Distribution allows subsurface flow and overland flow to be separately treated, allowing different delay modes, suitable for examining land cover impact on the stream hydrograph. As part of this development process, a new overland flow module has been established to represent the movement of surface water.

2.1 Subsurface flow module in a distributed TOPMODEL

Kirkby (1997) provided a classical approach to the rationale of TOPMODEL from the continuity equation based on strictly necessary assumptions. The development of our distributed subsurface flow module began from this point. As seen in Fig. 1, there is a flow strip with variable width in which the horizontal distance follows a curvilinear path down the line of greatest slope in a catchment, and the section with the length *dx* can be treated as a unit (i.e. calculating unit) in a distributed TOPMODEL.

Based on water balance, the general statement of hydrological continuity can be presented as Equation 1:

$$a\frac{\partial j}{\partial x} - \frac{\partial D}{\partial t} = (i - j)$$

Equation 1

where i is net rainfall intensity and j is discharge per unit area (i.e. runoff rate).

Equation 2 expresses the logarithmic assumption of the soil transmissivity profile in the original TOPMODEL (Kirkby, 1997):

$$D = -m \cdot \ln\left(aj / \Lambda q_0\right)$$

Equation 2

where D is soil moisture deficit; m is a scaling parameter which is assumed to be invariant over the flow strip and over time and shows how quickly discharge falls off with depth; aj is discharge per unit contour width and Λ is the tangent slope gradient. With $D = 0$ at soil saturation, q_0 is the discharge per unit width at saturation on unit slope gradient, and it may spatially vary in the catchment without violating the other assumptions. The runoff required to produce local saturation can be defined here. Setting $D = 0$ in Equation 2, it gives

$$j_* = \frac{\Lambda q_0}{a}$$

Equation 3

where j_* is discharge per unit area at saturation.

Substituting Equation 3 back into Equation 2, the formulation of j can be written as

$$j = j_* \cdot exp(-\frac{D}{m})$$

Equation 4

where *m* is again the soil depth parameter.

Transforming Equation 2, we get:

$$\frac{\partial D}{\partial t} = -\frac{m}{j} \cdot \frac{\partial j}{\partial t}$$

Equation 5

Combining Equation 1 and Equation 5, we have:

$$a\frac{\partial j}{\partial x} + \frac{m}{j} \cdot \frac{\partial j}{\partial t} = (i - j) \cdot$$

Equation 6

If *i* and *j* are assumed spatially uniform in a unit, the hydrological continuity within a cell can be expressed by Equation 7, and a solution can be obtained as Equation 8. Equation 6 is the more general form of Equation 7 which remains valid if *i* and *j* vary spatially:

$$\frac{dj}{dt} = \frac{j(i - j)}{m}$$

Equation 7

$$\ln\left(\frac{j}{i - j}\right) = \frac{it}{m} + C$$

Equation 8

where *C* is an unknown constant derived from initial conditions. At $t = 0$, $j = j_0$, substituting in Equation 8, *C* is solved as Equation 9:

$$C = \ln\left(\frac{j_0}{i - j_0}\right)$$

Equation 9

Combining Equation 9 with Equation 8 then gives Equation 10:

$$\ln\left(\frac{j}{i - j}\right) = \frac{it}{m} + \ln\left(\frac{j_0}{i - j_0}\right)$$

Equation 10

and, rearranging, to give the runoff *j,*

$$j = \frac{j_0}{\frac{j_0}{i} + (1 - \frac{j_0}{i}) \cdot exp(-\frac{it}{m})}$$

Equation 11

Equation 11 is the expression of j for a cell at time t within a time interval.

From Equation 4, D can be calculated by Equation 12:

$$D = m \cdot \ln\left(\frac{j_*}{j}\right)$$

Equation 12

Hence, if D_0 is defined as deficit at $t=t_0$ and D_1 is deficit at the end of time interval, we get

$$D_0 = m \cdot \ln\left(\frac{j_*}{j_0}\right)$$

Equation 13

$$D_1 = m \cdot \ln\left(\frac{j_*}{j_1}\right)$$

Equation 14

where j_1 is discharge per unit area at the end of a time interval.

In terms of water balance (i.e. net rainfall plus decrease of deficit equals runoff), total runoff in a time interval is expressed by Equation 15:

$$TF = i \cdot \Delta t + (D_1 - D_0) = m \ln\left(1 + \frac{j_*}{i} exp\left(-\frac{D_0}{m}\right) \cdot \left(exp\left(\frac{i \cdot \Delta t}{m}\right) \quad 1\right)\right)$$

Equation 15

where TF is total runoff for a cell, and Δt is the time interval.

However, Equation 15 should be implemented without modification only in the case for which the cell is never over-saturated (i.e. overland flow is never produced) in the time interval, because Equation 13 and Equation 14 (from Equation 4 and previously Equation 2) are defined to express runoff below the land surface and are hence only applicable for subsurface flow. In the case where saturation is reached within a time interval Δt, it is assumed that net rainfall intensity is constant during the time interval, and heavy enough to saturate the cell and produce overland flow at some time t_* within the time interval. If we suppose, at time t*, the soil just reaches saturation (i.e. deficit just equals zero and the total runoff rate is discharge at saturation, j_*), we have Equation 16 from Equation 11:

$$j_* = \frac{j_0}{\frac{j_0}{i} + (1 - \frac{j_0}{i}) \cdot exp(-\frac{it_*}{m})}$$

Equation 16

Solving it gives Equation 17 which is valid during the time interval, if $i > j_* > j_0$:

$$t_* = \frac{m}{i} \ln\left(\frac{j_*(i - j_0)}{j_0(i - j_*)}\right)$$

Equation 17

Before t_*, the cell is not at saturation, the moisture deficit is continuously decreasing and there is no overland flow, so that Equation 15 is applicable. Hence, substituting Equation 17 into Equation 15, the amount of subsurface flow from $t = 0$ to $t = t_*$ is

$$SSF_1 = m \ln\left(1 + \frac{j_*}{i} \cdot \left(\frac{j_*(i - j_0)}{j_0(i - j_*)} - 1\right)\right) = m \ln\left(\frac{i - j_0}{i - j_*}\right)$$

Equation 18

Between t_* and the end of time interval, the cell is continuously saturated due to the assumed continuing rainfall at the constant rate for the time step, and consequently the subsurface flow rate consistently equals j_* in this period. Subsurface flow in this stage is

$$SSF_2 = j_* \cdot (\Delta t - t_*)$$

Equation 19

In addition to subsurface flow, the surplus net rainfall transforms to saturation-excess overland flow whose amount is determined by Equation 20, and this is also the total overland flow within the time step:

$$SOF = i \cdot (\Delta t - t_*) - SSF_2 = (i - j_*) \cdot (\Delta t - t_*)$$

Equation 20

Total subsurface flow in the time interval is the sum of that in the two sub-stages (shown as Equation 21):

$$SSF = m \ln\left(\frac{i - j_0}{i - j_*}\right) + j_* \cdot (\Delta t - t_*)$$

Equation 21

The deficit at the end of the time step is zero due to its saturation at that point.

The case of a continuously saturated cell (i.e. the cell status which starts at saturation and undergoes large net rainfall, so that the cell remains saturated during the whole time interval) can be treated as a particular situation in the saturated case as above. The subsurface flow is calculated from the density of discharge at saturation through the time interval, leaving the other part of runoff as overland flow.

All equations for subsurface flow in a cell, which is the base of the distributed modification for TOPMODEL, have now been derived, and they will be used in the module for subsurface water behaviour and overland flow generation. The root zone and unsaturated zone components from the original TOPMODEL are still contained within the distributed TOPMODEL. However, the unsaturated zone delay is very short in peat due to high wetness and shallow water table, so the impact of the unsaturated zone delay is very limited for upland peatlands studied in this paper.

2.2 Overland flow module in a distributed TOPMODEL

The runoff delay in the original version of TOPMODEL was treated via a lumped method using a constant general channel flow velocity and a hillslope velocity. Field measurements in blanket peat have shown that overland flow may be significantly slower than assumed in the original TOPMODEL (Holden *et al.*, 2008), so that overland flow re-infiltrates downslope after a significant time delay. This delayed input partially violates the TOPMODEL assumption of spatially uniform rainfall input. Hence it is required that a delay is formed from a more explicit overland flow routine.

In order to simulate the overland flow movement and the surface cover impacts upon it, an overland flow module was developed, being a new component of a distributed TOPMODEL. After determining the overland flow volume from every cell in the model, the overland flow module controls the computation of spread and concentration of overland flow and derives the time consumed in this process. Routed overland flow water can then be re-involved in the hydrological calculation in down-flow slope cells (i.e. re-infiltration process), providing delayed local inputs to combine with subsequent rainfall in a spatially variable pattern. In the representation of overland flow, the time delay is calculated separately for each cell that generates or receives surface flow, providing an interactive relationship between subsurface flow and overland flow. The calculation unit is grid cell in order to suit the general spatial pattern of the DEM data.

2.2.1 Overland flow routing algorithm

The main assignment of the overland flow routing algorithm is to provide an overland flow distribution for every step of simulation and to support the calculation of overland flow delay. The multiple-direction flow algorithm is employed as a theoretical base to represent the overland flow routing procedure in the overland flow module. This routing algorithm is a multiple direction flow version of the D8 (deterministic eight node) algorithm (O'Callaghan and Mark, 1984) which on its own allocates all flow to the grid neighbouring cell with the steepest slope after considering the slopes to all eight neighbouring cells. The multiple-direction flow algorithm, however, which was firstly developed by Quinn *et al.* (1991), instead allows flow dispersion in hillslope routing processes. The water in a cell is split to its every lower neighbour cell and the fractions of water amount are determined by slope weights. The fraction of flow given to the neighbour n is given by Equation 22:

$$Fr_n = \frac{S_n}{\sum_{i=n}^{8} S_n}$$

Equation 22

where n is from 1 to 8 representing the eight directions of eight cells S_n is the gradient in direction n, and Fr_n is the flow fraction in direction n. The DEM data should be modified in advance with a pond-filling process in which the elevation of every cell with no lower neighbour cells is increased to the average value of its neighbours' elevations, since the pond water is not the issue this model wants to tackle. Meanwhile, a ranking procedure based on elevation value in the modified DEM map is firstly needed for all cells in the catchment. The Quick Sort Algorithm (Hoare, 1962; Sedgewick, 1978) is used to sort the cells in decreasing order of elevation value as a preparation before the entire hydrological calculation in the model. The routing algorithm is used for every cell in a time step throughout the whole period of the simulation. In each time step the model algorithm runs through every cell in the area, beginning with the highest cell (i.e. the peak point in the catchment) and ending with the lowest one (i.e. the outlet of the basin after the pond filling). This sequencing is required to ensure that all overland flow produced by higher cells has been included in the calculation for lower cells in the catchment during the same time step.

Within each time step the calculation for an individual cell begins by applying the rainfall, together with any overland flow from upslope, to estimate the infiltration, overland flow production, subsurface flow and updated local saturation deficit using a local solution to Equation 1. These processes themselves do not require the algorithm which then routes the overland flow, part of which may remain in the source cell and part distributed over cells downslope.

Two methods of routing the overland flow have been conceptualised. In the first the flow is repeatedly split between all adjacent downslope cells according to the distribution between alternative flow directions, setting up a chain reaction which is computationally inefficient to implement and difficult to parameterise. Alternatively the overland flow generated in each source cell is split into a number of parcels (50-100 or more), each a realisation of the total overland flow which is then followed stochastically, using the flow partitions (Equation 22) as the basis for selecting a path at random from cell to cell. The velocity of each parcel is calculated from the overland flow depth and the local gradient at each step of the flow path, using Manning's equation (Equation 25). The velocity calculated in this way is then interpreted as the probability that the path will terminate within the time step in each cell traversed. When all parcels have been followed to the ends of their respective paths, they are combined (and weighted) to give the destination distribution for all the overland flow generated in the source cell at the end of the time step.

The stop condition in the routing process for a single water parcel is also probabilistic. At each step along the path of an overland flow parcel, the velocity, v, is calculated from Equation 25, in which the depth is the depth of flow generated in the source cell and the gradient is the local gradient between successive cells on the flow path. It follows that, for this step, the mean travel distance in a time step δt is $v\delta t$. Applying an exponential distribution which is equivalent to assuming a constant probability of stopping per unit distance, the probability of stopping within one cell, of dimension δx (i.e. stopping within the current cell) may be written as $P = 1-\exp[-\delta x/(v\delta t)]$ and the outcome determined randomly. Water parcels after the routing process from a cell can stop in many downslope cells which cover a relatively extensive area with various flow path distances. Therefore, this leads to a consecutive and smooth distribution of overland flow travel distance for a cell, which helps to smooth out rapidly fluctuating runoff concentrations downslope. This stochastic algorithm has been preferred to the more complex chain reaction process, and implemented within the model code. Fig. 2 provides an example of the distributions of overland flow parcels from three individual source cells on hillslopes after a time step (6 min) in a modelling run. The source cells of overland flow were selected to demonstrate the algorithm, and overland flow from each source cell is separated into 10000 water parcels, each of which go through the algorithm to determine a location after the current time step in the model. For the cell on the top or middle of hilslopes (e.g. a and c), most parcels stop on the near downstream cells of the source cell after a time step even though there is a wide spread of overland flow parcels. This is because overland flow velocity in these locations is quite slow. It should be noted that the green cells in the figures only represent one to ten parcels (i.e. the magnitude of 0.01% - 0.1% of all overland flow from the source cell) so some individual parcels moving to very far downstream positions from the sources can only represent small probability events due to the stochastic algorithm of overland flow routing. The overland flow parcels from the source cell at the bottom of hilslopes (e.g. b) concentrate on cells further from the source cells after a time step, as the flow paths of these parcels are at the bottom of hillslopes and in river channels in which the overland flow velocity is much higher than that on top and middle of hillslopes.

After running through all cells (from high to low) in the catchment, the overland flow in the outlet cell is the overland flow output of the catchment in the current time step. This flow includes overland flow produced in current time steps in the area near the outlet and in former steps at longer distances away from it. Overland flow in the hillslope cells can lead to overland flow output or be part of subsurface flow output due to re-infiltration.

2.2.2 Time delay process and its equations

The time delay for water movement on hillslopes is generated by the down-flow accumulation of cell to cell delays, estimated from the velocity variations induced by acceleration and friction, which are themselves driven by topographic factors and land surface features. The equations for delay time of overland flow (or the equations for velocity of overland flow) should therefore be related to surface gradient, flow depth, and land surface cover. The Darcy-Weisbach equation (as Equation 23) can be utilized as an expression of land surface resistance to overland flow, which provides a theoretically-based way to build relationships among overland flow velocity, gradient, flow depth and the friction factor in upland peatlands backed up by empirical observations (Holden *et al.*, 2008):

$$v^2 = \frac{8g}{f} dS$$

Equation 23

where S is the surface slope and, v is the mean velocity of overland flow, d is overland flow depth, g is gravitational acceleration, and f is the dimensionless friction factor. f can be related to the ratio of water depth, d to an effective roughness diameter, k, which can be described by an empirical equation (Equation 24):

$$\frac{1}{\sqrt{f}} = A + 1.77 \ln\left(\frac{d}{k}\right)$$

Equation 24

where A is an empirically defined constant.

Combining Equation 23 and Equation 24, overland flow velocity will be related to flow depth and slope gradient with a couple of constants but the expression may be complex. From the work of Holden *et al.* (2008), when we have $10 < d/k < 10000$ there is a relationship of $f^{-0.5} \sim (d/k)^{1/6}$ which is consistent with Manning's equation. Thus we can simplify to:

$$v = k_v \cdot d^{2/3} \cdot S^{1/2}$$

Equation 25

where k_v is a suitable constant based on Equation 23 and Equation 24. This is a succinct form of a velocity calculation in which water depth will be obtained in every cell at every time step during model runs. Gradient can be gained through an analysis of elevation data before the hydrological simulation.

The algorithms describing overland flow movement have been presented in this section. The new model therefore has the ability to represent land-cover change impacts on overland flow in a fully distributed fashion. We now test the model for an upland peatland.

3 Study site

The Trout Beck catchment (54°41' N, 2°23' W) is situated at Moor House National Nature Reserve (also a World Biosphere Reserve) in the North Pennine region of northern England, covering an area of 11.4 km^2 (see Fig. 3). It is one of the headwaters of the River Tees, with an elevation ranging from 842 m to 533 m AOD. Hourly river flow and weather data from 1993 to 2009 was obtained for the site. Around 90% of the catchment is covered by blanket peat with a typical depth of 1-2 m (Evans *et al.*, 1999). The peat suffered widespread erosion in the 1950s, but large areas have re-vegetated with *Sphagnum* and *Eriophorum* since then (Grayson *et al.*, 2010). A *Calluna-Eriophorum* association dominates the vegetation cover of the catchment, and in areas above 630 m AOD, *Eriophorum* alone becomes dominant (Evans *et al.*, 1999).

The climate of the catchment is classified as sub-arctic oceanic (Manley, 1942), with an annual average temperature (1931–2006) of 5.3 ℃ (Holden and Rose, 2011), and a mean annual rainfall of 2012 mm (records from 1951 to 1980 and 1991 to 2006) (Holden and Rose, 2011). 43% of the annual precipitation falls between April to September (Grayson *et al.*, 2010).

4 Model calibration and validation

4.1 Method and model setting

The GLUE method of Beven and Binley (1992) rejects the concept of an optimum or best parameter set for a system, and all parameter sets are assumed to have an equal likelihood of being acceptable estimators of the system. The existence of multiple behavioural parameter sets is a generic modelling problem in the face of uncertainty (Cameron *et al.*, 1999). From a specified parameter space, many parameter sets are picked using Monte Carlo simulation, evaluated by likelihood measures and some are rejected as non-behavioural after the assessment. This framework is now widely used to estimate uncertainty and evaluate results in hydrological modelling (e.g. Freer *et al.*, 1996; Aronica *et al.*, 2002).

For the distributed TOPMODEL, the number of simulation runs for calibration and validation must be limited, because the distributed model can have a long run time. Thus, the three crucial parameters of m, K, and k_v in the distributed TOPMODEL were only taken into account in the test process. m is the active depth for subsurface flow; K is a 'notional' hydraulic conductivity of soil in the model ($K \times m$ is the transmissivity); k_v is the velocity parameter of overland flow. Due to the shortage of field observations of these parameters, they were assumed to be homogeneous throughout the catchment for the purposes of the test.

The experience from other TOPMODEL applications (Beven, 1997; Kirkby, 1997) can be used to narrow the parameter space and so restrict the number of calibration runs needed. In order to avoid uneven distribution of parameter sets in parameter space caused by such a limited number of runs, the parameter sets were scanned systematically in the parameter space (as shown in Table 1), giving 90 sets of parameters for calibration.

Comparing the simulated hydrographs with the observed one, the Nash-Sutcliffe efficiency (the measure of likelihood) of each simulation result was calculated. The top 20% of simulated hydrographs with the highest efficiency are then used to compose an envelope band of hydrographs which is compared to the observed runoff through the calibration period. These top 20% parameter sets were picked to run the model through the validation period. The same top 20% of parameter sets were then used to created envelope bands of the validation storm and compared to the observed hydrograph of the validation period.

To avoid freezing and melting problems and the lower reliability of winter precipitation records due to snowfall, rainfall events for model calibration and validation were selected from summer-half years (from 1993 to 2009). Fig. 4 summarises the yearly maximum hourly summer rainfall. A one-week period commencing from 16th August 2004 (105 mm total rainfall) has been chosen as a suitable period for calibration. It includes a storm event with 19.4 mm precipitation in one hour which represents an approximately 10-year return period estimated from the empirical frequency of events (Fig. 4). Another wet week near to the calibration period is selected as the validation period commencing from 8th August 2004 (128 mm total rainfall). The Penman-Monteith equation is employed to estimate potential evapotranspiration during the calibration and validation periods. It is assumed that actual evapotranspiration is equal to potential evapotranspiration, as peat soil is very wet and there is plentiful water for evapotranspiration in the catchment.

4.2 Results of calibration and validation

For the flow calibration, the Nash-Sutcliffe efficiency for each simulation run was computed to measure the likelihood, and the top 20% hydrograph band is plotted in Fig. 5. The top 20% of parameter sets in the calibration were run in the model during the validation period and the band of resulting hydrographs is illustrated in Fig. 6. The two hydrograph bands of calibration and validation span most of the observed hydrographs in the two periods. The Nash-Sutcliffe efficiency for the single best-fitted hydrograph, the upper boundary of the band, and the lower boundary of the band were calculated to represent the model performance during both the calibration and validation periods (Table 2). The model performance was satisfactory since the Nash-Sutcliffe efficiency of the top 20% simulations in the calibration is over 0.78, and that in validation is more than 0.64. This test result demonstrates that the distributed TOPMODEL can simulate runoff well for the Trout Beck catchment.

4.3 Comparison of the distributed TOPMODEL and the original TOPMODEL

To compare the distributed TOPMODEL to the original TOPMODEL, the same modified GLUE procedure was applied to the Trout Beck catchment data with the same storm events for calibration and validation, applying the original version of TOPMODEL. The physical means of m and K were the same as those in the distributed TOPMODEL. *V* is the uniform velocity of runoff. All three parameters are homogenous for the catchment due to the lumped configuration of the original TOPMODEL. Parameter ranges of *m* and *K* are kept from the test in the distributed TOPMODEL, and Table 3 shows the parameter space for the original TOPMODEL, in which there are 90 parameter sets.

The hydrograph band constituted from the top 20% efficiency results for the calibration runs is illustrated in Fig. 7. Using these top 20% parameter sets the hydrograph band was produced from validation runs (Fig. 8) and Table 4 shows the Nash-Sutcliffe efficiency of the hydrograph bands in the calibration and validation.

Comparing the test results of the distributed TOPMODEL and the original TOPMODEL, the calibration hydrograph bands are quite similar for the two models. The Nash-Sutcliffe efficiency of the highest fitted hydrograph and the upper boundary in the results of the original TOPMODEL is slightly better than the distributed model. However, for the validation results, the hydrograph band of the distributed TOPMODEL envelopes more parts of the observed hydrograph. The Nash-Sutcliffe efficiency of all three representative curves for the band of the distributed TOPMODEL is distinctly better than that for the original TOPMODEL. The two envelopes in the calibration and validation periods for the distributed TOPMODEL bracket 50.0% and 68.5% of the observations respectively (Fig. 5 and Fig. 6), and for the original TOPMODEL they are 37.6% and 42.8% (Fig. 7 and Fig. 8). This comparison implies that the new distributed TOPMODEL performed better than the original version in this catchment, and the distributed configuration and the new overland flow module seem to improve the model's ability to predict river flow. Clearly this is in addition to the benefits developed including the spatial distribution and the fact that users of the new model can also determine overland flow volumes and velocities across any point in the catchment for each time step used.

However, the cost of the distributed model is time of model runs. The simulation of the distributed TOPMODEL takes about 20 min per run (a simulation week) using an Intel i7 Processor (4 core 2.0 GHz), while the original one takes less than 2 seconds for a run. In the distributed TOPMODEL, actual running time consumed for an individual modelling time step mainly depends on the overland flow contributing area which is related to the rainfall amount in the current time step and the overland flow contributing area formed in the previous time steps. A larger contributing area means that more cells are under calculation for the overland flow routing and re-infiltration in the overland flow module, and that, for an individual cell in the contributing area, the overland flow route has a greater chance of being extended. These distributed overland flow calculations are more time-consuming than the subsurface flow calculation.

In terms of the key parameters used in the two models, the transmissivity (T_0) has a large difference between models. The range of transmissivity in the original TOPMODEL is 100 – 300 $m^2\ hr^{-1}$ while it is 0.3 – 5.4 $m^2\ hr^{-1}$ in the distributed TOPMODEL. As indicated by Wigmosta and Lettenmaier (1999), effective transmissivity values predicted by the original TOPMODEL are higher than the simulated result given by a subsurface flow kinematic wave solution. On the other hand, higher transmissivity leads to more subsurface flow. Around 80% of runoff is subsurface flow in the calibration period in the simulations of the original TOPMODEL, and this proportion of subsurface flow seems to be too high for blanket peatland catchments, in which peak runoff should be dominated by surface or very near-surface flow (Holden and Burt, 2002). However, this situation is different for the distributed TOPMODEL. Only about 20% of runoff is subsurface flow during the calibration period in the simulations of the distributed TOPMODEL. Thus, it may be inferred that the development of the distributed TOPMODEL improves the physical meanings of the model with respect to blanket peat headwaters.

A scenario was employed to demonstrate the difference between simulated soil moisture deficit for the two models. The example shown in Fig. 9 was run for 100 time steps with a rainfall input which consists of a 1-hour storm with 20 mm hr^{-1} rate at time step 11. A parameter set having high efficiency (over 0.8) in the calibration and validation was chosen to run the distributed TOPMODEL and the same values of K (hydraulic conductivity) and m (scaling parameter) were also used in the original TOPMODEL for comparison. The overland flow velocity parameter (V) of the original TOPMODEL was optimized to match the resulting hydrograph with that of the distributed TOPMODEL. The simulation runs of the two models start with a same outlet flow value from which the moisture deficit distribution at the first modelling time step is derived for both runs of the two models. Fig. 9 shows the resulting hydrographs of the two models for this scenario.

At the time step 10 (just before the rainfall input), the values of soil moisture deficit and their spatial distributions for the two models are quite similar (as shown in Fig. 10 (a) and (d)). This is because both of the models applied the same mechanism of subsurface flow simulation even though the distributed structure is adopted in the new model. At the time step just after the rainfall event (time step 12), the soil moisture deficit within the simulation of the distributed TOPMODEL is lower than that within the original TOPMODEL (see Fig. 10 (b) and (e)). Hence there are wetter hillslopes in the distributed TOPMODEL than those in the original one due to the reinfiltration mechanism. After rainfall, the soil moisture deficit of the two simulations both decrease step by step after the storm. Fig. 10 (c) and (f) illustrate that the moisture deficit of the distributed model simulation is still larger than that within the original model at time step 40 but the difference between them is less than that in the earlier time step just after the rainfall.

From the above scenario modelling, we can show that re-infiltration mechanisms in the distributed TOPMODEL decrease soil moisture deficit after storm events as more surface water infiltrates into soil during the process of overland flow movement on hilslopes. At the same time, overland flow delay on hillslopes in the model provides more ‘opportunities’ to overland flow for re-infiltration. These changes in the distributed TOPMODEL should result in improvements to peak flow modelling. Güntner *et al.* (1999), compared simulated runoff components from the original TOPMODEL and those derived from hydrograph separation by tracer investigations and field observations during two storm events in a German mountainous forested basin (Brugga basin, 40 km^2). The modelled saturation-excess overland flow reached peaks earlier than the real saturation-excess overland flow, and the peak contributions of simulated saturation-excess overland flow were larger than those of measured event water. Their work highlighted a deficiency of the original TOPMODEL but our distributed version of TOPMODEL makes significant improvements through the overland flow delay and re-infiltration mechanisms. The overland flow routing process in the new model provides a reasonable delay of overland flow movement on hillslopes and makes a part of saturation-excess overland flow contribute to the recession part of peak hydrographs. This accords with the findings of Güntner *et al.* (1999), in which the exchange between surface and subsurface water and the flow source and path was recommended for future catchment hydrological modelling.

5 Model sensitivity to land-cover change and future applications

The new model was designed to describe the land cover impact on overland flow movement, so it should be sensitive to varying land cover types. Three scenarios, representing bare peat, *Eriophorum* cover and *Sphagnum* cover (which are three typical land cover types in the Trout Beck catchment) respectively covering the whole catchment, were performed as preliminary test of the model sensitivity to land-cover change. The parameter set used in the *Eriophorum* scenario was picked up in the calibration and validation procedure (the efficiency of the set is over 0.8), in which the land cover was assumed to be uniform over the catchment, as the Trout Beck catchment is primarily dominated by *Eriophorum* (Evans *et al.*, 1999). The other two scenarios used the same parameters in the set except for the overland flow velocity parameter. Using the empirical research of Holden *et al.* (2008) the overland flow velocity parameter in bare peat is five times greater than for *Eriophorum*, while the overland flow velocity parameter in *Sphagnum* is half that of *Eriophorum.* A one hour rainfall pulse with a uniform rate of 20 mm hr^{-1} (i.e. 2 mm per 6-min), which is similar to the one in 10-year summer rainfall event (Fig. 4) was the precipitation input in model runs used for the sensitivity test. The modelling time step was set as 0.1 hr (6 min) to examine differences in flow peak time and magnitude between cover type scenarios.

The outlet hydrographs of the three scenarios are illustrated in Fig. 11, indicating that there are large differences among the results. If we considered the *Eriophorum* scenario as a standard, the bare peat scenario produces a 46.3 % higher and a 5-step earlier peak than the *Eriophorum* scenario while the *Sphagnum* one gives a 40.3 % lower and 6-step later peak than the standard one. This implies that the model is sensitive to the overland flow velocity parameter which is associated with land cover type.

6 Conclusions

This paper has developed novel work to transform the traditional TOPMODEL into a distributed differential model, retaining classical key ideas on runoff production but focusing on land-cover change impacts on overland flow velocities leading to river flow hydrographs. The new model is totally distributed with a computational unit of a grid cell. In the new distributed model, the impacts of land-cover change on in-situ water movement and downstream river flow can both be represented and simulated by this model improvement. At the same time, the distributed model has another crucial advantage in that it can represent the spatial variability of precipitation for rainfall-runoff simulations. The spatial variability of rainfall can greatly affect the timing and shape of peak flow hydrographs (Wilson *et al.*, 1979; Syed *et al.*, 2003), no matter which scale of catchment is being investigated (e.g. 4-5 ha. Faures *et al.*, 1995). On the other hand, rainfall variability in space can also produce problems in calibrating hydrological models (Arnaud *et al.*, 2002). Distributed hydrological models allow the distribution pattern of rainfall input to be provided in the model. This means every cell can be assigned rainfall inputs for every time step, which is a disaggregated way to describe the spatial and temporal variability of rainfall. Thus, the model can utilise more accurate precipitation data (e.g. from rainfall radar) to decrease the negative influence of rainfall spatial variability on flow modelling. Of course the availability of distributed rainfall data is a practical problem for many upland sites but it is thought that such data availability will improve over time and thus the model is ready and fit-for-purpose for future flow modelling in upland systems.

A new module, with a series of distributed algorithms representing water routing and velocity, models the movement of overland flow and the surface cover impact on overland flow. After the overland flow routing process, a water parcel stops at a downstream cell in which it is treated as input water for the cell and may infiltrate into the soil to contribute to subsurface flow produced in this cell or it may add to further overland flow production associated with changes in flow depth for the cell for the given time step. This mechanism reflects the real process of overland flow generation on hillslopes and may be influenced by land cover. Land-cover change decreases or increases transportation time for overland flow and thus decreases or increases the opportunity for the infiltration of overland flow. This interactive hillslope overland flow-infiltration mechanism represented in the distributed TOPMODEL is rarely considered in catchment hydrological models. A similar mechanism can only be found in a few hydrological modelling studies such as the work of Wang *et al.* (2011) by which the mechanism was used in the model for rainfall-runoff simulations for a macro-scale (> 10000 km^2) catchment with a resolution of 1-km grid cells or rather larger than the hillslope scale overland flow process. At the same time as providing this significant new advance which could have wide applicability, there is only one key parameter (k_v the parameter of overland flow velocity) which has been added for overland flow compared to the constant overland flow velocity parameter in the original TOPMODEL, limiting the possibilities of over-parameterization (Perrin *et al.*, 2001). The small number of parameters required to run the model is an obvious benefit for the application of the model, and makes it easier to calibrate and validate in practice.

The model was found to be very sensitive to land cover type. Therefore it can be used in future studies which test different spatially-distributed scenarios of land-cover change which upland peatland managers are concerned about. These concerns may include removal of vegetation (e.g. by erosion processes, pollution, overgrazing) or good revegetation of peat with sedges such as *Eriophorum* or mosses such as *Sphagnum*. It should be possible to conduct experiments with the model to test for optimum locations, concentrations and sizes of land-cover change in order to reduce flood peaks.

Acknowledgements

We would like to thank the China Scholarship Council and the School of Geography of the University of Leeds for funding this project. We are also grateful to the UK's Environmental Change Network for provision of data.

References

Arnaud P, Bouvier C, Cisneros L, Dominguez R. 2002. Influence of rainfall spatial variability on flood prediction. Journal of Hydrology, **260**: 216-230. DOI: 10.1016/s0022-1694(01)00611-4.

Aronica G, Bates PD, Horritt MS. 2002. Assessing the uncertainty in distributed model predictions using observed binary pattern information within GLUE. Hydrological Processes, **16**: 2001-2016. DOI: 10.1002/hyp.398.

Ballard CE, McIntyre N, Wheater HS, Holden J, Wallage ZE. 2011. Hydrological modelling of drained blanket peatland. Journal of Hydrology, **407**: 81-93. DOI: 10.1016/j.jhydrol.2011.07.005.

Beven K. 1997. TOPMODEL: A critique. Hydrological Processes, **11**: 1069-1085. DOI: 10.1002/(sici)1099-1085(199707)11:9<1069::aid-hyp545>3.0.co;2-o.

Beven K, Binley A. 1992. The future of distributed models - model calibration and uncertainty prediction. Hydrological Processes, **6**: 279-298. DOI: 10.1002/hyp.3360060305.

Beven KJ, Kirkby MJ. 1979. A physically-based variable contributing area model of basin hydrology. Hydrological Sciences Bulletin, **24**: 43-69.

Beven KJ, Kirkby MJ, Schofield N, Tagg AF. 1984. Testing a physically-based flood forecasting-model (Topmodel) for 3 UK catchments. Journal of Hydrology, **69**: 119-143. DOI: 10.1016/0022-1694(84)90159-8.

Bower MM. 1962. The cause of erosion in blanket peat bogs. Scottish Geographical Magazine, **78**: 33-43.

Bragg OM, Tallis JH. 2001. The sensitivity of peat-covered upland landscapes. Catena, **42**: 345-360. DOI: 10.1016/s0341-8162(00)00146-6.

Cameron DS, Beven KJ, Tawn J, Blazkova S, Naden P. 1999. Flood frequency estimation by continuous simulation for a gauged upland catchment (with uncertainty). Journal of Hydrology, **219**: 169-187. DOI: 10.1016/s0022-1694(99)00057-8.

Evans MG, Burt TP, Holden J, Adamson JK. 1999. Runoff generation and water table fluctuations in blanket peat: evidence from UK data spanning the dry summer of 1995. Journal of Hydrology, **221**: 141-160. DOI: 10.1016/s0022-1694(99)00085-2.

Evans R. 2005. Curtailing grazing-induced erosion in a small catchment and its environs, the Peak District, Central England. Applied Geography, **25**: 81-95. DOI: 10.1016/j.apgeog.2004.11.002.

Faures JM, Goodrich DC, Woolhiser DA, Sorooshian S. 1995. Impact of small-scale spatial rainfall variability on runoff modeling. Journal of Hydrology, **173**: 309-326. DOI: 10.1016/0022-1694(95)02704-s.

Franks SW, Gineste P, Beven KJ, Merot P. 1998. On constraining the predictions of a distributed moder: The incorporation of fuzzy estimates of saturated areas into the calibration process. Water Resources Research, **34**: 787-797. DOI: 10.1029/97wr03041.

Freer J, Beven K, Ambroise B. 1996. Bayesian estimation of uncertainty in runoff prediction and the value of data: An application of the GLUE approach. Water Resources Research, **32**: 2161-2173. DOI: 10.1029/95wr03723.

Güntner A, Uhlenbrook S, Seibert J, Leibundgut C. 1999. Multi-criterial validation of TOPMODEL in a mountainous catchment. Hydrological Processes, **13**: 1603-1620.

Gallego-Sala AV, Prentice IC. 2013. Blanket peat biome endangered by climate change. Nature Climate Change, **3**: 152-155. DOI: 10.1038/nclimate1672.

Grayson R, Holden J, Rose R. 2010. Long-term change in storm hydrographs in response to peatland vegetation change. Journal of Hydrology, **389**: 336-343. DOI: 10.1016/j.jhydrol.2010.06.012.

Hess TM, Holman IP, Rose SC, Rosolova Z, Parrott A. 2010. Estimating the impact of rural land management changes on catchment runoff generation in England and Wales. Hydrological Processes, **24**: 1357-1368. DOI: 10.1002/hyp.7598.

Hoare CAR. 1962. Quicksort. Computer Journal, **5**: 10-16. DOI: 10.1093/comjnl/5.1.10.

Holden J. 2005. Peatland hydrology and carbon release: why small-scale process matters. Philosophical Transactions of the Royal Society a-Mathematical Physical and Engineering Sciences, **363**: 2891-2913. DOI: 10.1098/rsta.2005.1671.

Holden J, Burt TP. 2002. Infiltration, runoff and sediment production in blanket peat catchments: implications of field rainfall simulation experiments. Hydrological Processes, **16**: 2537-2557. DOI: 10.1002/hyp.1014.

Holden J, Burt TP. 2003. Runoff production in blanket peat covered catchments. Water Resources Research, **39**. DOI: 10.1029/2002wr001956.

Holden J, Chapman PJ, Labadz JC. 2004. Artificial drainage of peatlands: hydrological and hydrochemical process and wetland restoration. Progress in Physical Geography, **28**: 95-123. DOI: 10.1191/0309133304pp403ra.

Holden J, Kirkby MJ, Lane SN, Milledge DG, Brookes CJ, Holden V, McDonald AT. 2008. Overland flow velocity and roughness properties in peatlands. Water Resources Research, **44**. DOI: 10.1029/2007wr006052.

Holden J, Rose R. 2011. Temperature and surface lapse rate change: a study of the UK's longest upland instrumental record. International Journal of Climatology, **31**: 907-919. DOI: 10.1002/joc.2136.

Holden J, Shotbolt L, Bonn A, Burt TP, Chapman PJ, Dougill AJ, Fraser EDG, Hubacek K, Irvine B, Kirkby MJ, Reed MS, Prell C, Stagl S, Stringer LC, Turner A, Worrall F. 2007b. Environmental change in moorland landscapes. Earth-Science Reviews, **82**: 75-100. DOI: 10.1016/j.earscirev.2007.01.003.

Immirzi CP, Maltby E, Clymo RS. 1992. The global status of peatlands and their role in carbon cycling. In: A report for Friends of the Earth by the Wetland Ecosystems Research Group, Dept Geography, University of Exeter, pp: 1-145.

IUCN. 2011. IUCN UK Commission of Inquiry on Peatlands. In: IUCN UK Peatland Programme.

Kirkby MJ. 1976. Chapter 3 Hydrograph modelling strategies. In: Processes in Physical and Human Geography, Peel R, Chisholm M, Haggett P (eds.) Heinemann.

Kirkby MJ. 1997. TOPMODEL: A personal view. Hydrological Processes, **11**: 1087-1097. DOI: 10.1002/(sici)1099-1085(199707)11:9<1087::aid-hyp546>3.0.co;2-p.

Lamb R, Beven K, Myrabo S. 1998. Use of spatially distributed water table observations to constrain uncertainty in a rainfall-runoff model. Advances in Water Resources, **22**: 305-317. DOI: 10.1016/s0309-1708(98)00020-7.

Lane SN, Milledge DG. 2013. Impacts of upland open drains upon runoff generation: a numerical assessment of catchment-scale impacts. Hydrological Processes, **27**: 1701-1726. DOI: 10.1002/hyp.9285.

Manley G. 1942. Meteorological observations on Dun Fell, a mountain station in northern England. Quarterly Journal of the Royal Meteorological Society, **68**: 151-165.

O'Callaghan JF, Mark DM. 1984. The extraction of drainage networks from digital elevation data. Computer Vision Graphics and Image Processing, **28**: 323-344. DOI: 10.1016/s0734-189x(84)80011-0.

Parrott A, Brooks W, Harmar O, Pygott K. 2009. Role of rural land use management in flood and coastal risk management. Journal of Flood Risk Management, **2**: 272-284. DOI: 10.1111/j.1753-318X.2009.01044.x.

Parry LE, Holden J, Chapman PJ. 2014. Restoration of blanket peatlands. Journal of Environmental Management, **133**: 193-205. DOI: http://dx.doi.org/10.1016/j.jenvman.2013.11.033.

Perrin C, Michel C, Andreassian V. 2001. Does a large number of parameters enhance model performance? Comparative assessment of common catchment model structures on 429 catchments. Journal of Hydrology, **242**: 275-301. DOI: 10.1016/s0022-1694(00)00393-0.

Peters NE, Freer J, Beven K. 2003. Modelling hydrologic responses in a small forested catchment (Panola Mountain, Georgia, USA): a comparison of the original and a new dynamic TOPMODEL. Hydrological Processes, **17**: 345-362. DOI: 10.1002/hyp.1128.

Price JS. 1992. Blanket bog in Newfoundland. Part 2. Hydrological processes. Journal of Hydrology, **135**: 103-119. DOI: 10.1016/0022-1694(92)90083-8.

Quinn P, Beven K, Chevallier P, Planchon O. 1991. The prediction of hillslope flow paths for distributed hydrological modeling using digital terrain models. Hydrological Processes, **5**: 59-79. DOI: 10.1002/hyp.3360050106.

Sedgewick R. 1978. Implementing quicksort programs. Communications of the Acm, **21**: 847-857. DOI: 10.1145/359619.359631.

Syed KH, Goodrich DC, Myers DE, Sorooshian S. 2003. Spatial characteristics of thunderstorm rainfall fields and their relation to runoff. Journal of Hydrology, **271**: 1-21. DOI: 10.1016/s0022-1694(02)00311-6.

Wang JH, Yang H, Li L, Gourley JJ, Sadiq IK, Yilmaz KK, Adler RF, Policelli FS, Habib S, Irwn D, Limaye AS, Korme T, Okello L. 2011. The coupled routing and excess storage (CREST) distributed hydrological model. Hydrological Sciences Journal-Journal Des Sciences Hydrologiques, **56**: 84-98. DOI: 10.1080/02626667.2010.543087.

Wheater H, Evans E. 2009. Land use, water management and future flood risk. Land Use Policy, **26**: S251-S264. DOI: 10.1016/j.landusepol.2009.08.019.

Wigmosta MS, Lettenmaier DP. 1999. A comparison of simplified methods for routing topographically driven subsurface flow. Water Resources Research, **35**: 255-264. DOI: 10.1029/1998wr900017.
Wilson CB, Valdes JB, Rodriguez-Iturbe I. 1979. Influence of the spatial-distribution of rainfall on storm runoff. Water Resources Research, **15**: 321-328. DOI: 10.1029/WR015i002p00321.

Tables

Table 1. Parameter space for the model calibration.

Parameter	Parameter ranges		
	Lower value	Upper value	Increment
m (m)	0.003	0.018	0.003
k_v	10	50	10
K (m hr^{-1})	100	300	100

Table 2. Nash-Sutcliffe efficiency of the hydrograph band in the calibration and validation

Hydrograph	Calibration efficiency	Validation efficiency
Highest fitted hydrograph	0.851	0.833
Upper boundary	0.833	0.778
Lower boundary	0.785	0.644

Table 3. Parameter space for the calibration of the original TOPMODEL.

Parameter	Parameter ranges		
	Lower value	Upper value	Increment
m (m)	0.003	0.018	0.003
V (m hr^{-1})	800	1600	200
T_0 (m^2 hr^{-1})	100	300	100

Table 4. Nash-Sutcliffe efficiency of the hydrograph band in the calibration and validation for the original TOPMODEL.

Hydrograph	Calibration efficiency	Validation efficiency
Highest fitted hydrograph	0.860	0.797
Upper boundary	0.853	0.772
Lower boundary	0.683	0.533

Figure list

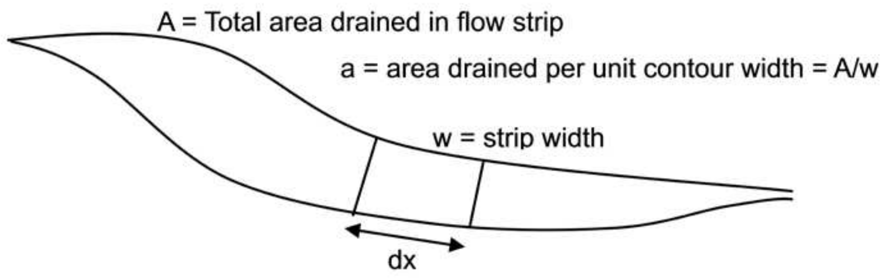

Fig. 1. Definition sketch for flow strip (after Kirkby, 1997). x is horizontal distance.

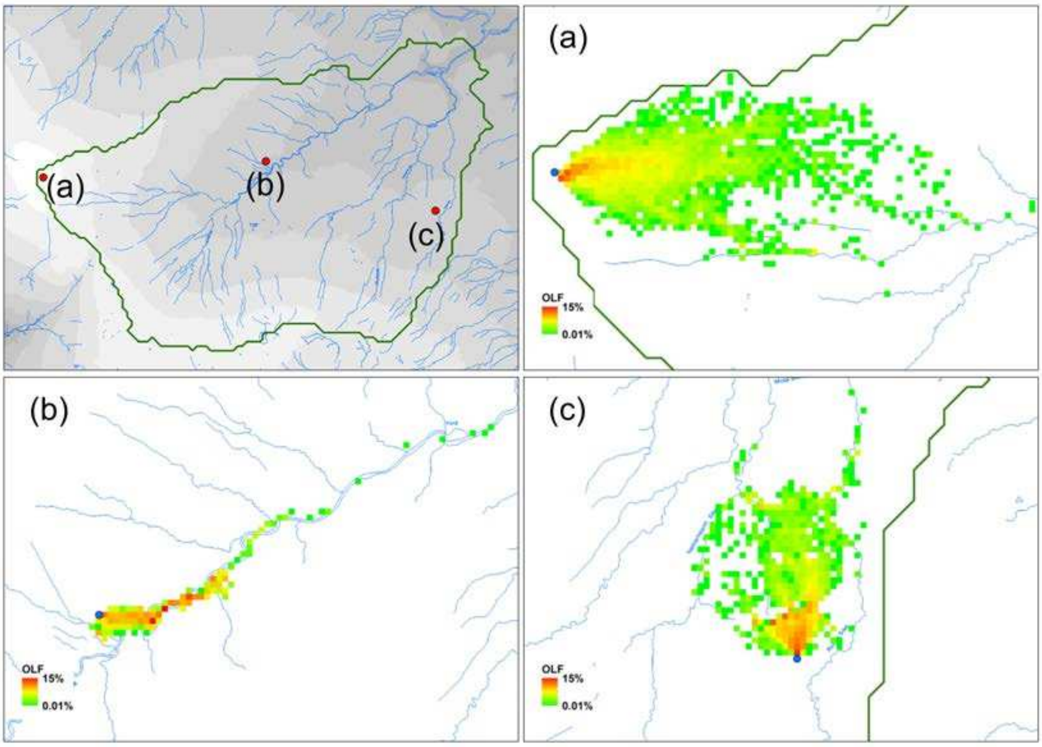

Fig. 2. The distributions of water parcels from three individual source cells (a, b and c) on hillslopes after a time step. (The scale of overland flow percentage in the legend is logarithmic).

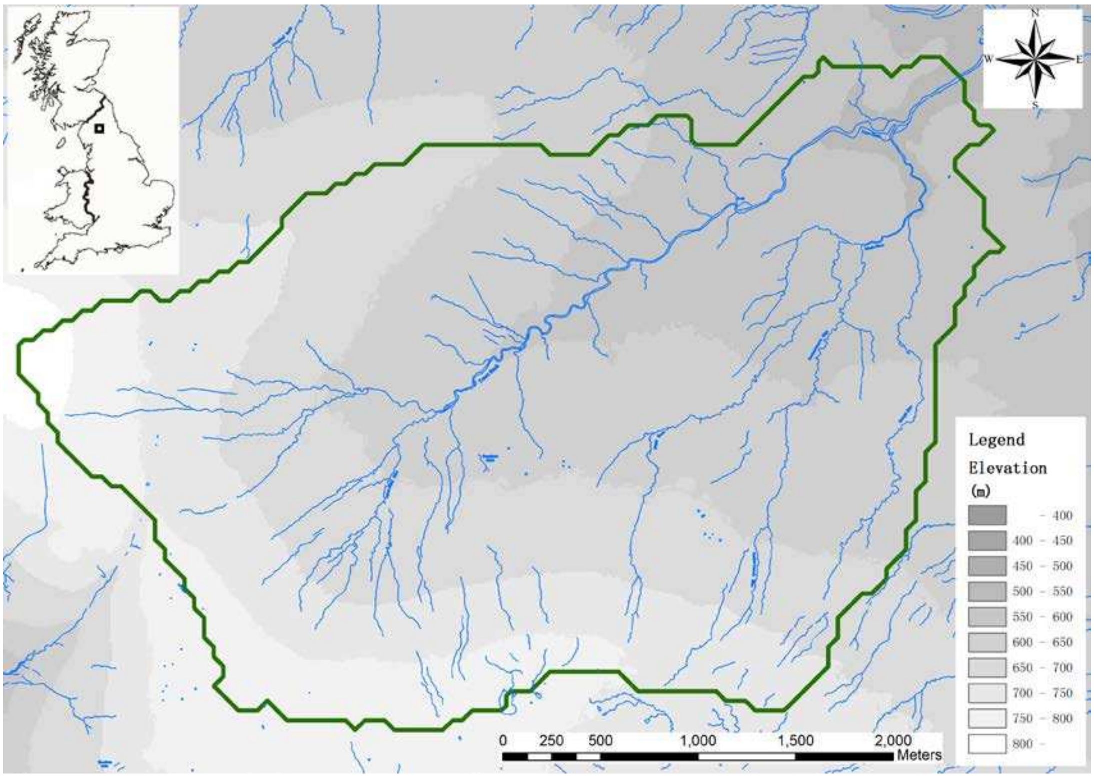

Fig. 3. Location and map of the Trout Beck catchment.

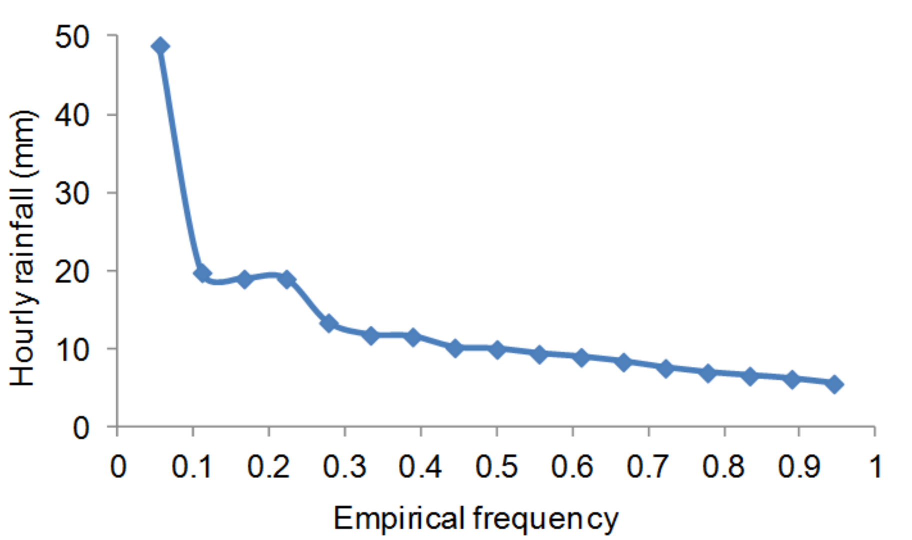

Fig. 4. Observed frequency of hourly rainfall intensities of yearly maximum from 1993 to 2009.

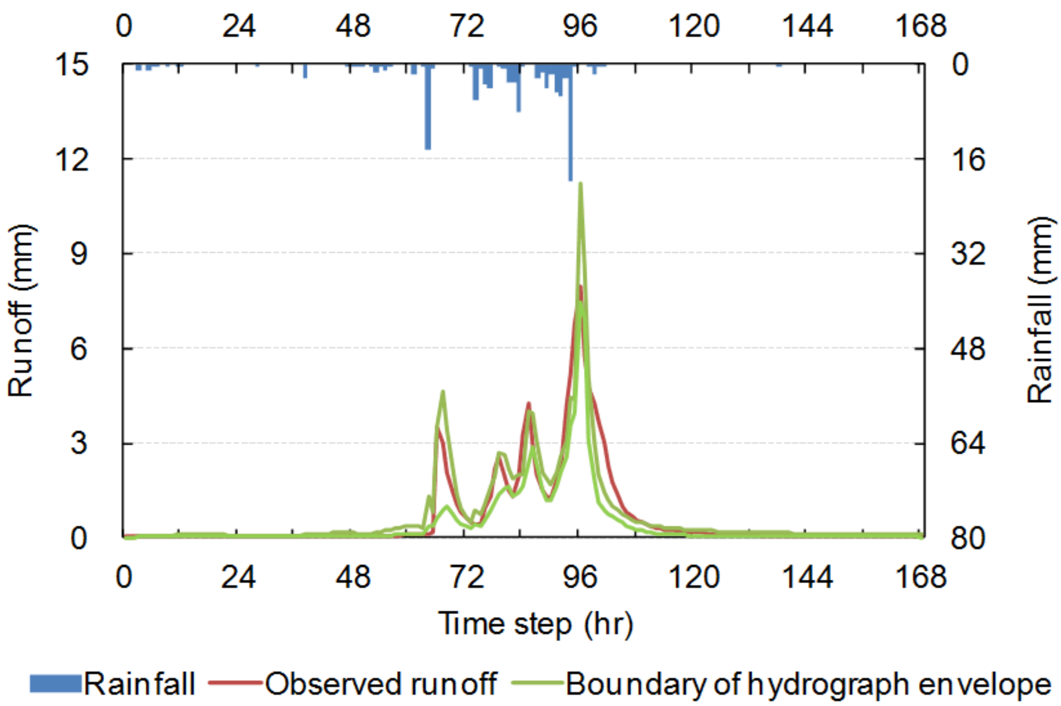

Fig. 5. Comparison of the observed runoff and the top 20% simulation hydrograph band in the calibration period.

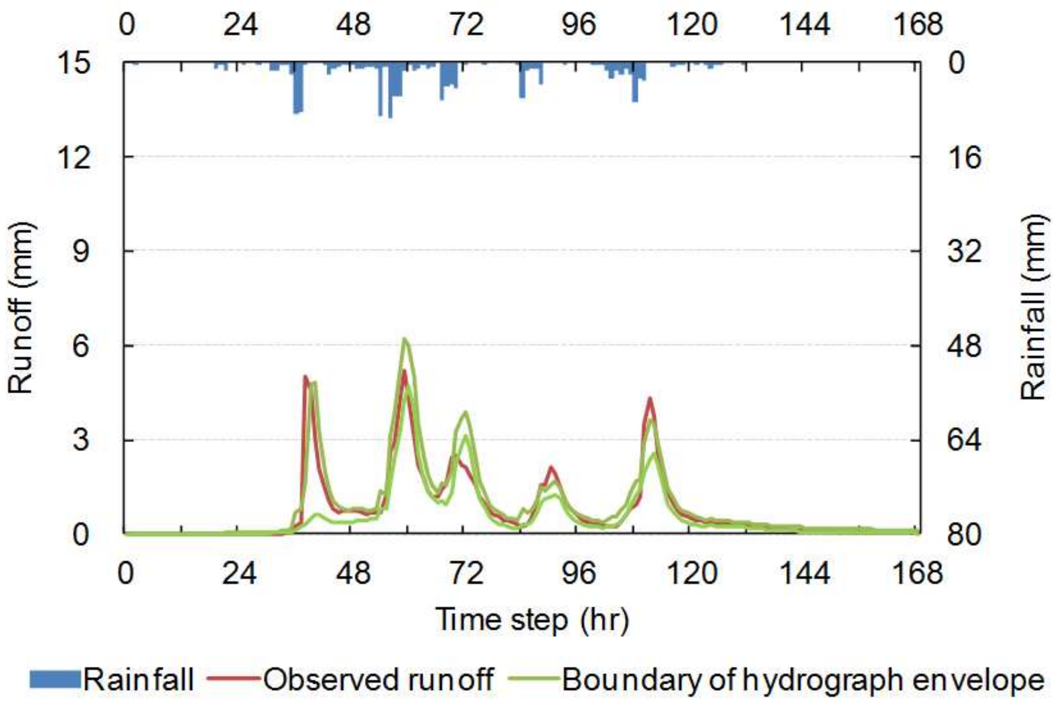

Fig. 6. Comparison of the observed runoff and the hydrograph band in the validation period.

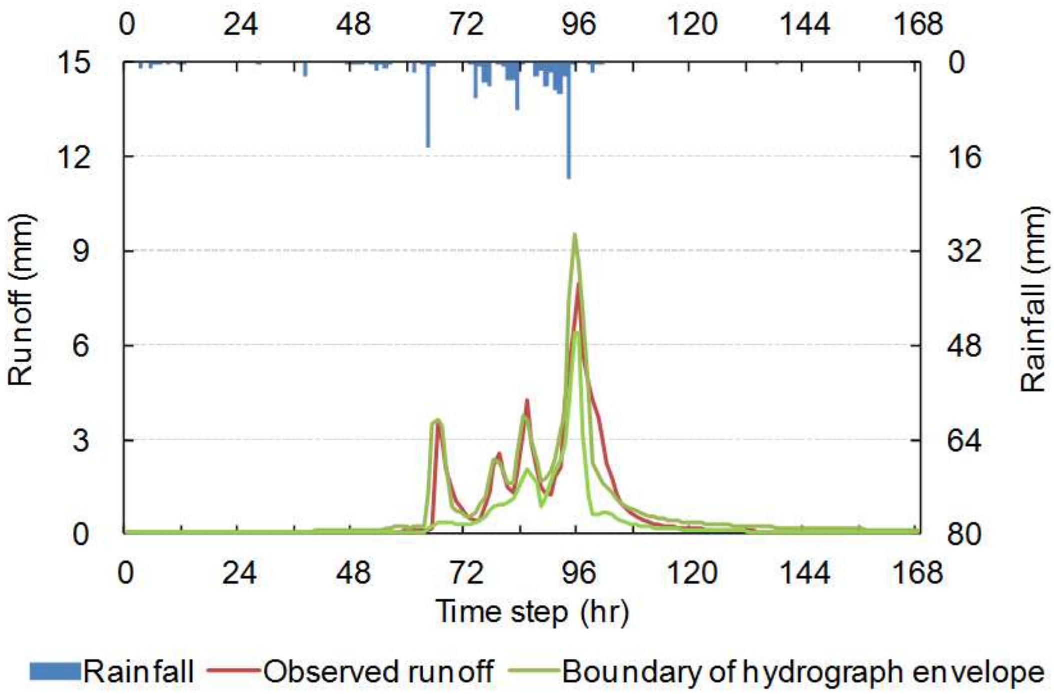

Fig. 7. Comparison of the observed runoff and the top 20% simulation hydrograph band in calibration period for the original TOPMODEL.

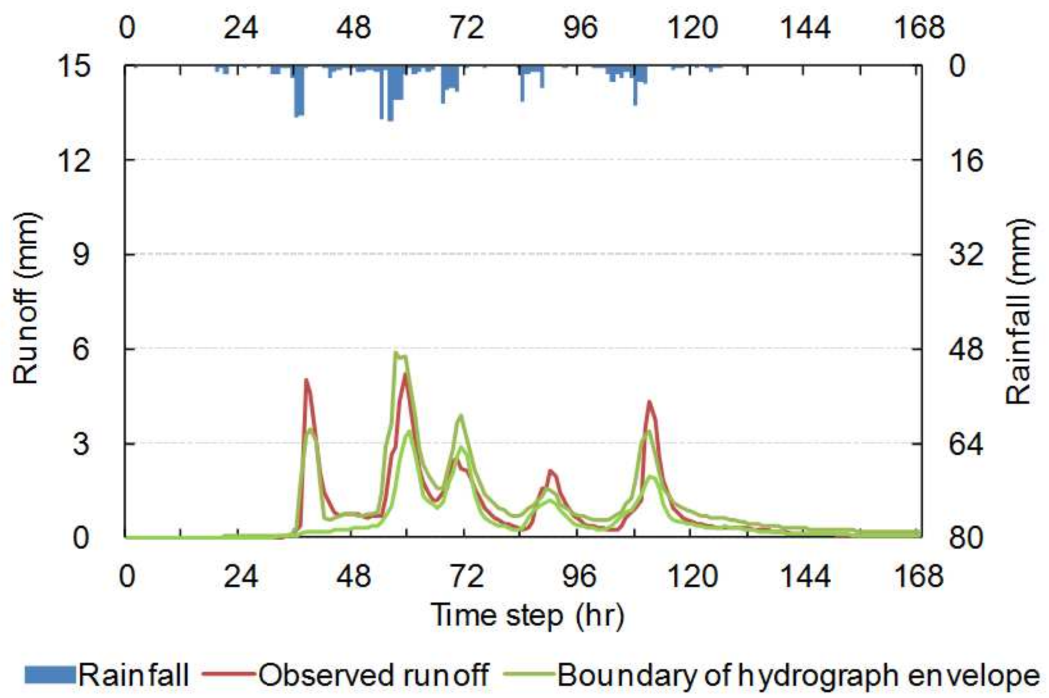

Fig. 8. Comparison of the observed runoff and the hydrograph band in validation period for the original TOPMODEL.

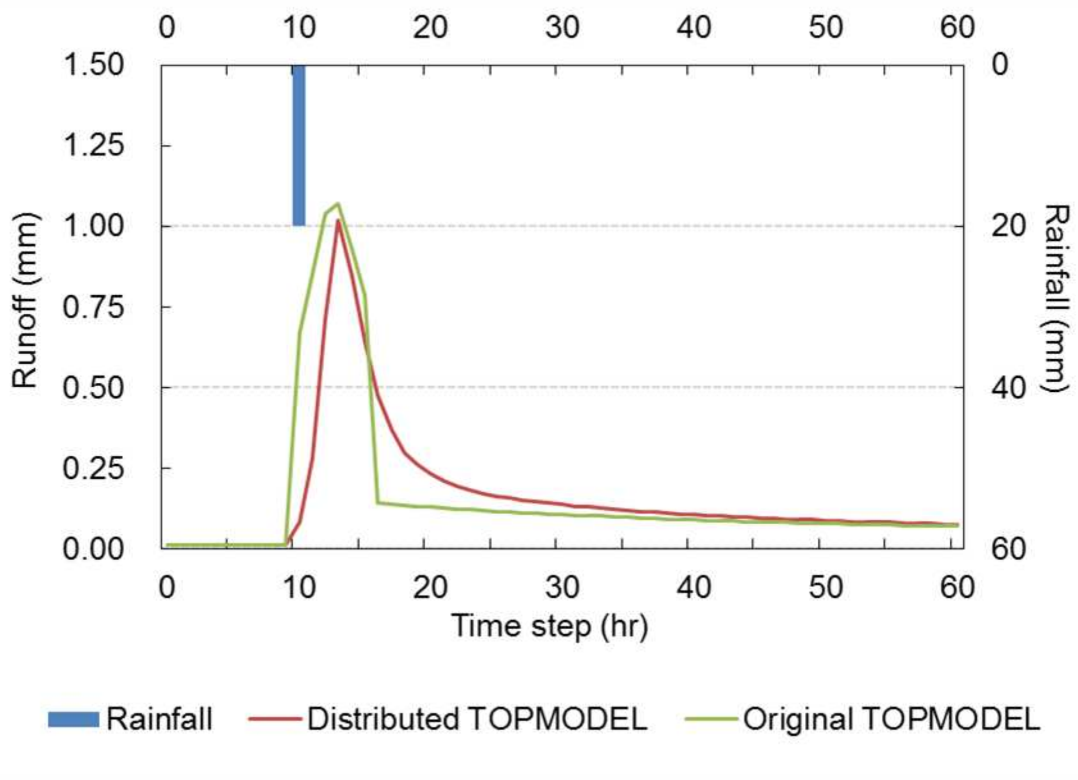

Fig. 9. Hydrographs of the scenario of soil moisture deficit comparison for the distributed TOPMODEL and the original TOPMODEL.

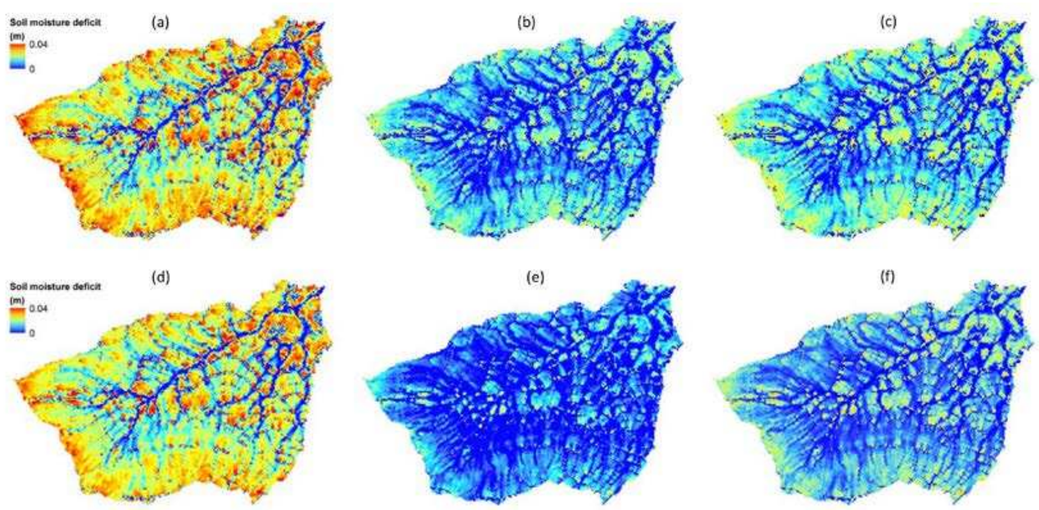

Fig. 10. Distribution of soil moisture deficit in the scenario modelling; (a), (b) and (c) represent the simulated distribution of soil moisture deficit at time step 10, 12 and 40 respectively from the original TOPMODEL, while (d), (e) and (f) represent the simulated distribution of soil moisture deficit at time step 10, 12 and 40 respectively from the distributed TOPMODEL.

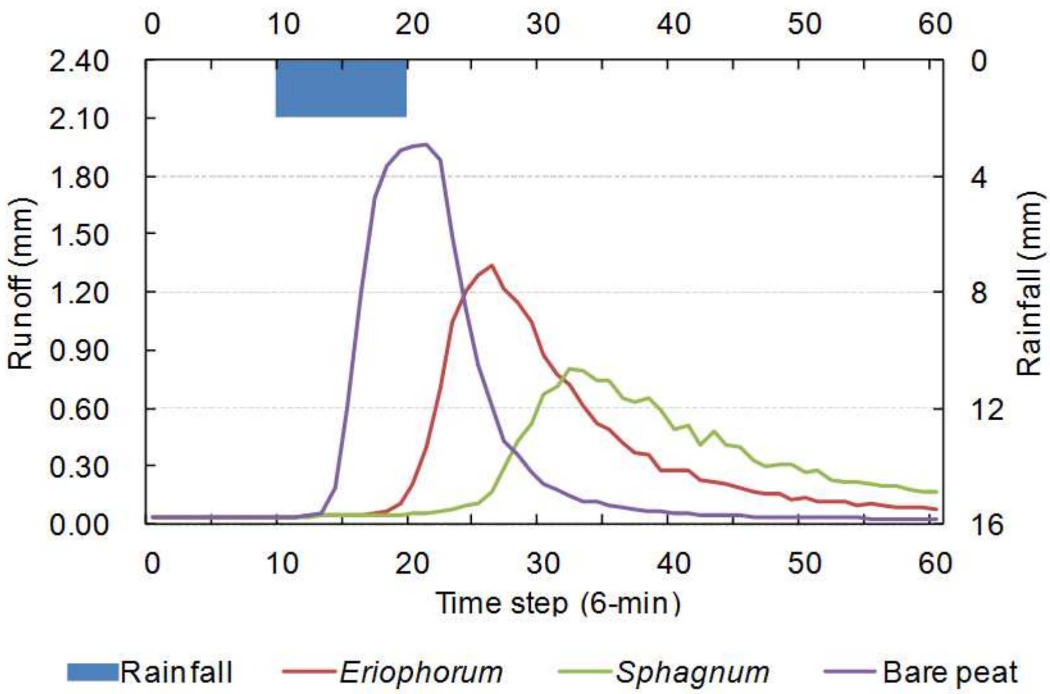

976

977 Fig. 11. Modelling responses of three typical vegetation covers under a 1-
978 hour 20-mm rainfall event for the test of model sensitivity.